[6] Spreiter, J. R. and Stahara, S. S., "Developments in Transonic Flow Theory," *Zeitschrift für Flugwiss* 18, Heft 2/3, 1970, pp. 33–40.

[7] Spreiter, J. R., Alksne, A. Y., and Hyett, B. J., "Theoretical Pressure Distributions for Several Related Nonlifting Airfoils at High Subsonic Speeds," TN 4148, 1958, NACA.

[8] Spreiter, J. R., "On the Application of Transonic Similarity Rules to Wings of Finite Span," Rept. 1153, 1953, NACA (supersedes NACA TN 2726).

# Determination of Axial Gradient Effects in Freejet Flows

A. G. Keel Jr.* and R. N. Zapata†
*University of Virginia, Charlottesville, Va.*

### Nomenclature

$C_{D\text{nose}}$ = value of drag coefficient based on parameters at model nose
$d_0$ = nominal diameter of source orifice
$D$ = model base diameter
$Kn_{ri}(r_n)$ = $\lambda_{ri}/r_n$
$L$ = model length
$M_{is}$ = isentropic axial Mach number
$Re_{w,L}$ = $\rho_\infty U_\infty L/\mu_w$, where $\mu_w$ is viscosity coefficient based on $T_w$
$r_n, r_B$ = radius of model nose, radius of model base
$T_w$ = model wall temperature
$U_\infty$ = freestream (axial) velocity
$\langle v_r \rangle$ = $2(2RT_w/\pi)^{1/2}$, mean thermal speed of reflected molecules
$\lambda_\infty$ = hard sphere mean-free-path of incident molecules
$\rho_{fip}$ = freestream value of incident stream density at first interaction point of reflected with incident molecule
$\rho_{\text{nose}}$ = freestream value of incident stream density at model nose
$\rho_\infty$ = freestream incident density
$\Delta\rho$ = axial variation in freestream density across model length
$\Psi$ = $r_n/r_B$, model bluntness ratio

### Introduction

In this Note an empirical technique for assessing the influence of axial flow gradients in free jets on the measurements of drag coefficients of slender, blunted cones at zero angle-of-attack is discussed. Specific results obtained for low-density flows are used to predict the values of the drag coefficient for the case of a uniform flow characterized by the flow parameters at the nose of the cones.

### Experimental Method

A schematic of the experimental apparatus is shown in Fig. 1. The freejet flow is produced by allowing gas to emerge from the stagnation chamber through a thin-plate orifice into a vacuum. The conical model is supported in midstream by an electromagnetic balance. A careful calibration procedure makes it possible to relate the magnitude of the current through the supporting coils to the magnitude of the aerodynamic force with high accuracy and precision.[1] The axial jet-core flow properties are a function of the axial position scaled with respect to the (effective) source orifice diameter.[2]

Received May 5, 1970; revision received June 19, 1970. Research supported by Grant AFOSR-69-1798. The assistance of R. D. Passmore in the data acquisition and reduction is gratefully acknowledged.

* Assistant Research Engineer.
† Associate Professor. Member AIAA.

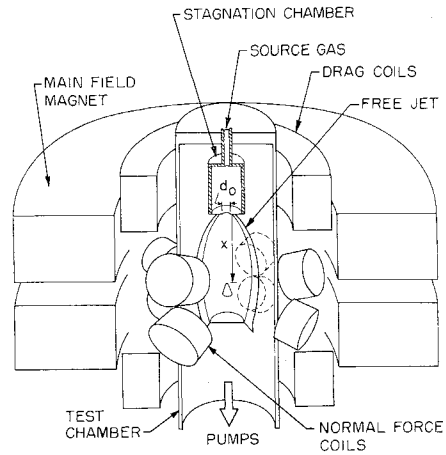


**Fig. 1 Schematic of experiment.**

To study the influence of flow gradients on the aerodynamic characteristics of cones, the magnitude of these gradients was varied by varying the size of the source orifice. By adjusting the axial position of the models in the freejet, the Mach number at the nose of the cones could be made the same in every case. A total of four source orifices and four models were used in this investigation (see Table 1). By varying the source pressure a range of the correlating flow parameter, $Re_{w,L}$, between 2.5 and 100 was obtained.

### Results and Discussion

Results of the tests for one model are plotted in Fig. 2 (three lower traces of solid symbols) as a family of curves of $C_D$ vs $Re_{w,L}$ for different magnitudes of the axial gradients of the freejet flow. An indication of the magnitude of the variation of the flow parameters over the length of the cones ($\Delta\rho/\rho_{\text{nose}}$) can be found in Table 1. From these and similar results obtained with other models two consistent trends emerge. First, in the higher $Re_{w,L}$ range the curves of a family are parallel and eventually become linear in the log-log plot. Second, as $Re_{w,L}$ is decreased, the curves in a family diverge, with the point of divergence occurring at a higher value of $Re_{w,L}$ when the flow gradients are steeper (i.e., the source orifice is smaller). These two trends suggest two distinct effects of flow gradients on the aerodynamics of a test body.

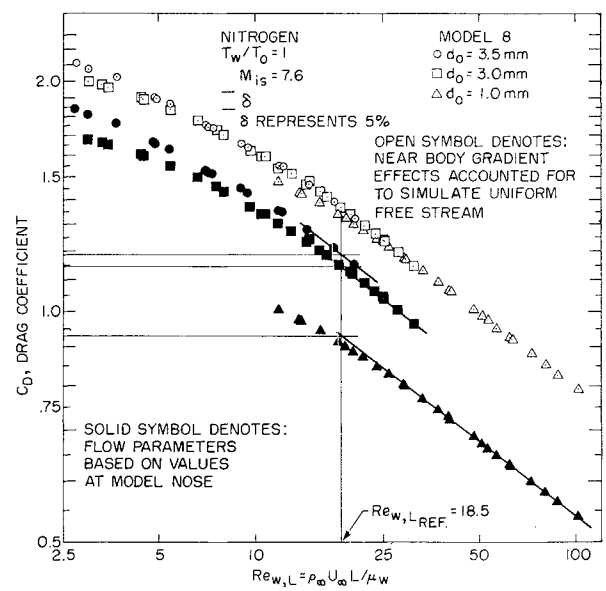


**Fig. 2 $C_D$ vs $Re_{W,L}$ for gradient flow and for corresponding uniform freestream.**

**Table 1 Summary of results**

| Model No. | $L$, mm | $D$, mm | $\psi = r_n/r_B$ | $d_0$, mm | $\Delta\rho/\rho_{\text{nose}}$ | $C_{D\text{nose}}$ @$Re_{w,L\text{ref}}$ | 1st departure point from parallel curves: $Re_{w,L}$ | $\rho_{fip}/\rho_{\text{nose}}$ @$\lambda_{ri}$ | $Kn_{ri}$ |
|---|---|---|---|---|---|---|---|---|---|
| 8 | 2.26 | 1.01 | 0.30 | 1.0 | 0.425 | 0.93 | 23.8 | 1.048 | 1.092 |
| | | | | 3.0 | 0.183 | 1.15 | 5.94 | 1.065 | 4.366 |
| | | | | 3.5 | 0.161 | 1.19 | | | |
| 7B | 4.93 | 2.12 | 0.25 | 2.0 | 0.449 | 0.94 | 24.8 | 1.051 | 1.310 |
| | | | | 3.0 | 0.342 | 1.06 | 14.5 | 1.058 | 2.239 |
| | | | | 3.5 | 0.307 | 1.11 | | | |
| 6 | 4.55 | 3.23 | 0.55 | 2.0 | 0.426 | 1.03 | 45.0 | 1.025 | 0.166 |
| | | | | 3.5 | 0.288 | 1.06 | | | |
| 3 | 4.52 | 2.26 | 0.45 | 2.0 | 0.425 | 0.92 | 25.0 | 1.046 | 0.784 |
| | | | | 3.5 | 0.287 | 1.02 | | | |

Semivertex angle = 9°

### *"Far body" effects*

The low $Re_{w,L}$ trend described previously is attributed to far body effects. At this point it is useful to keep in mind that that it is differences in the character of the flow-body interaction between the cases of uniform flow and gradient flow that are being examined, rather than attempting to explain the absolute nature of this interaction. For hypersonic flow the velocity of the stream is essentially constant leaving only the density as the pertinent "differencing" parameter characterizing the interaction between molecules reflected upstream from the body and the freestream particles. Considering only the "first interaction point," one mean-free-path upstream from the body nose (computed from conditions at the nose), the flow density will be higher for high gradient flows than for low gradient flows. This should result in a higher level of interaction between the reflected and the freestream molecules and, consequently, in a more severe departure from the drag produced by a uniform flow. To test this hypothesis, the mean-free-path of reflected molecules onto the incident stream is considered in the form

$$\lambda_{ri} \doteq 2^{1/2}\lambda_\infty/(U_\infty/\langle v_r\rangle + 1)$$

Next, the ratio of the freestream density one mean-free-path upstream from the model-nose to that at the model-nose, $\rho_{fip}/\rho_{\text{nose}}$, is computed. The observed correlation between the magnitude of this ratio and the point of departure from parallel behavior of the $C_D$ vs $Re_{w,L}$ curves is documented in Table 1. This correlation exhibits the proper dependence on the magnitude of $Kn_{ri}(r_n)$. For a larger value of $Kn_{ri}(r_n)$ it should take a larger magnitude of $\rho_{fip}/\rho_{\text{nose}}$ to produce a significant divergence of the $C_D$ vs $Re_{w,L}$ curves. This admittedly simple model of the far body interaction seems to be substantiated quite well by the experimental results.

To be sure, viscous and rarefaction effects in the jet core, and the low Reynolds number dependence of the effective orifice diameter could produce a low $Re_{w,L}$ behavior like the one observed. However, the magnitude of the observed effect, its somewhat dramatic nature, and the lack of any apparent nozzle Reynolds number correlation seems to indicate that the proposed "far body" effects are dominant.

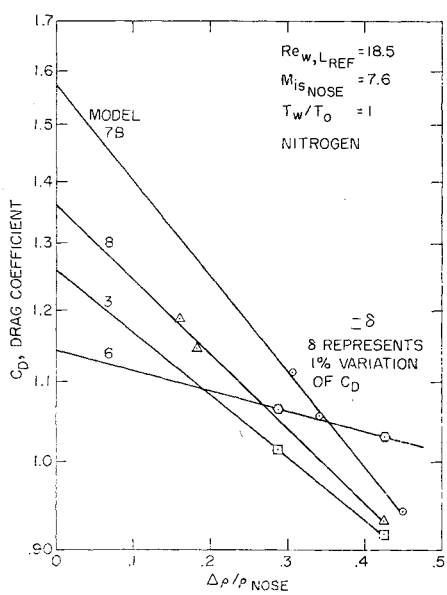


**Fig. 3 Drag coefficient vs flow property variation across model length for given value of $Re_{W,L}$.**

### *"Near body" effects*

The parallel displacement of the $C_D$ vs $Re_{w,L}$ curves in the higher $Re_{w,L}$ range is attributed to the variation of the freestream flow parameters across the length of the model. At sufficiently high values of $Re_{w,L}$, this near body effect is independent of the value of the freestream density over the range of parameters covered in this investigation. This suggests a straightforward empirical correction of the data with extrapolation to equivalent uniform freestream conditions. Starting with a family of curves for a given model (i.e., three lower plots in Fig. 2), a reference value of $Re_{w,L}$ is chosen. From each curve the value of $C_D$ for the chosen value of $Re_{w,L}$ is read. Next the values of $\Delta\rho/\rho_{\text{nose}}$ are computed for each case (see Table 1). Resulting plots of $C_D$ vs $\Delta\rho/\rho_{\text{nose}}$ are shown in Fig. 3 for four different models. For models 7B and 8 the least square fit of the experimental points yields a straight line within a maximum deviation of 0.5%. The intercepts of these straight lines with the ordinate should correspond to values of $C_D$ for an equivalent uniform freestream flow specified by the conditions of the actual flow at the model nose. Once these limiting values are obtained the actual data can be corrected for near body effects by parallel displacement of the curves, resulting in the upper curve of Fig. 2 for model 8. This correction at one value of $Re_{w,L}$ brings the curves together except over the range where far body effects become significant. Naturally, then, the simulation of uniform flow using a free expanding jet is valid only down to the value of $Re_{w,L}$ at which the onset of far body effects for the lowest gradient flow (largest source orifice) is felt.

The proposed method for interpreting experimental results obtained with freejet flows in terms of equivalent uniform flows appears to the authors to be far superior than attempting to correlate the data in terms of average values of the flow parameters. By placing models of different geometries at

identical initial (nose) freestream conditions, this method allows a direct comparison of results in terms of parameters based on these initial conditions.

### References

[1] Keel, A. G., Jr., "Low Density Hypersonic Cone Drag," Ph.D. dissertation, 1970, Dept. of Aerospace Engineering and Engineering Physics, Univ. of Virginia.

[2] Ashkenas, H. and Sherman, F. S., "The Structure and Utilization of Supersonic Free Jets in Low Density Wind Tunnels," *Rarefied Gas Dynamics*, Fourth Symposium, Supplement 3, Vol. II, 1966, pp. 84–105.

## Substructure Heating on Cracked Ablative Heat Shields

Eva M. Winkler,* Richard L. Humphrey,† Michael T. Madden,‡ and Joseph A. Koenig§
*U. S. Naval Ordnance Laboratory, White Oak, Silver Spring, Md.*

### Nomenclature

| | |
|---|---|
| $b$ | = crack width, typically 0.01 in. to 0.1 in. |
| $H_w$ | = wall enthalpy, Btu/lb |
| $H_0$ | = stagnation enthalpy, Btu/lb |
| $h$ | = crack height, in. |
| $\dot{m}$ | = ablation rate, lb/ft² sec |
| $\dot{m}/\rho_\infty u_\infty St$ | = blowing rate parameter |
| $q$ | = local heat transfer to crack wall, Btu/ft²sec |
| $q_s$ | = surface heat transfer, Btu/ft²/sec |
| $Re_\theta$ | = momentum thickness Reynolds number, $\rho_\infty u_\infty \theta/\mu_\infty$ |
| $Re_\tau$ | = friction Reynolds number, $(\tau_w/\rho)(\rho b/\mu)$ |
| $St$ | = Stanton number |
| $u_\infty$ | = freestream velocity, ft/sec |
| $\delta^*$ | = boundary-layer displacement thickness, in. |
| $\rho$ | = local density |
| $\rho_\infty$ | = freestream density |
| $\tau_w$ | = wall shear stress, lb/ft² |

### Introduction

ABLATIVE materials are used to protect re-entry vehicles from the intense heating during certain phases of the flight. However, if cracks develop in the heat shield prior to the re-entry, the substructure may be subjected to excessive heating. The ablative behavior of the heat shield may be altered in the vicinity of the cracks which in turn can affect the aerodynamics of the vehicle. The analytical description of the processes is inadequate to allow a safe design of heat shields. A moderate number of studies have been performed on non-ablating, shallow cavities and rectangular notches of various aspect ratios.[1] The present research program was formulated to look into this matter for ablating surfaces in high-speed flow. It was supplemented by independent analytical and experimental studies carried out by the Aeronautical Research Associates of Princeton, Inc.

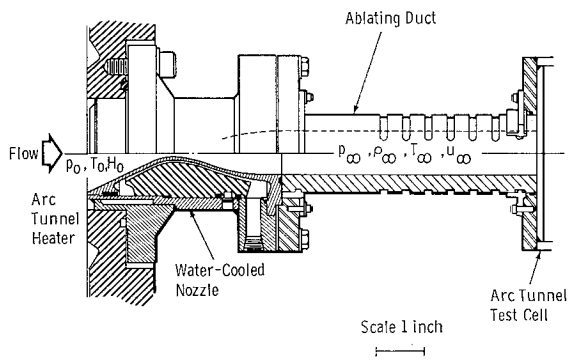


**Fig. 1 Schematic of experimental arrangement.**

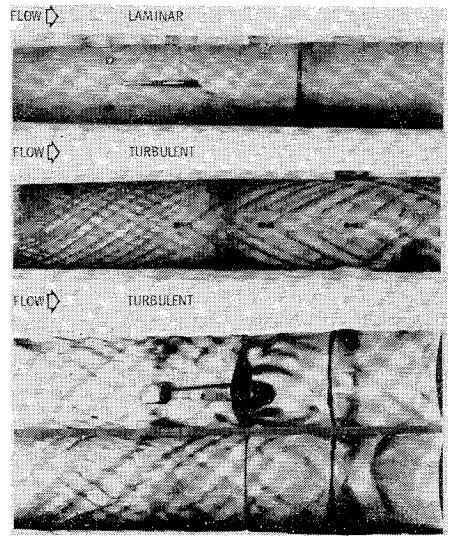


**Fig. 2 Striation patterns (top views of ducts cut in half after tests).**

### Approach

The present investigations are primarily experimental and were carried out in the Naval Ordnance Laboratory's (NOL) 3 Megawatt Arc Tunnel. They were designed for conditions that may occur at the conical part of a slender, blunted re-entry vehicle at an altitude of about 60,000 ft. Local Mach numbers between 2 and 3.5, enthalpy ratios $H_w/H_0$ of 0.2 to 0.4 and heating rates of about 200 to 300 Btu/ft² sec and Teflon as the ablator were chosen. Other parameters that were considered are the friction Reynolds number, $Re_\tau$, and characteristic sizes $b/\delta^*$ and $h/b$.

### Experiments

The arrangement is schematically shown in Fig. 1. Two axially symmetric nozzles designed for Mach numbers of 2.3 and 3 were used. The Teflon ducts were instrumented for pressure, in-depth wall temperature and skin-friction measurements. The cracks, up to three in one duct, were instrumented for heat-transfer measurements on the bottom, upstream and downstream walls.[2] For the Mach 3 run, the boundary layer was predicted to be laminar for a supply air pressure of 20 atm and a temperature of 9000°R. The turbulent boundary-layer tests were carried out at a Mach number of 2.3, pressures of 20 and 28 atmospheres and temperatures of 4600°R.

### Analytical Procedures

The laminar test results were compared with a numerical code,[3] which gives ablation rates, boundary-layer parameters and in-depth material responses for quasi-steady or transient conditions. For the turbulent data, a numerical procedure was devised that combines a computational program applicable to turbulent boundary layers on nonablating walls, experimental information, and wall-species and temperature data to correlate the substructure heating data.[2]

Received May 22, 1970; revision received July 6, 1970. This work was sponsored by the Defense Atomic Support Agency under Contract DASA 563-68.

* Supervisor, Aerospace Engineer.
† Aerospace Engineer. Member AIAA.
‡ Aerospace Engineer. Associate AIAA.
§ Aerospace Engineering Technician.